Electronic Supplementary Information (ESI) For

Proton Conductivity and Phase Transitions in 1,2,3-Triazole

Martin Pulst[a], Jens Balko[b], Yury Golitsyn[b], Detlef Reichert[b], Karsten Busse[a] and Jörg Kressler*[,a]

[a] Department of Chemistry, Martin Luther University Halle-Wittenberg, D-06099 Halle, Germany

E-mail: joerg.kressler@chemie.uni-halle.de

[b] Department of Physics, Martin Luther University Halle-Wittenberg, D-06099 Halle, Germany

X-ray data

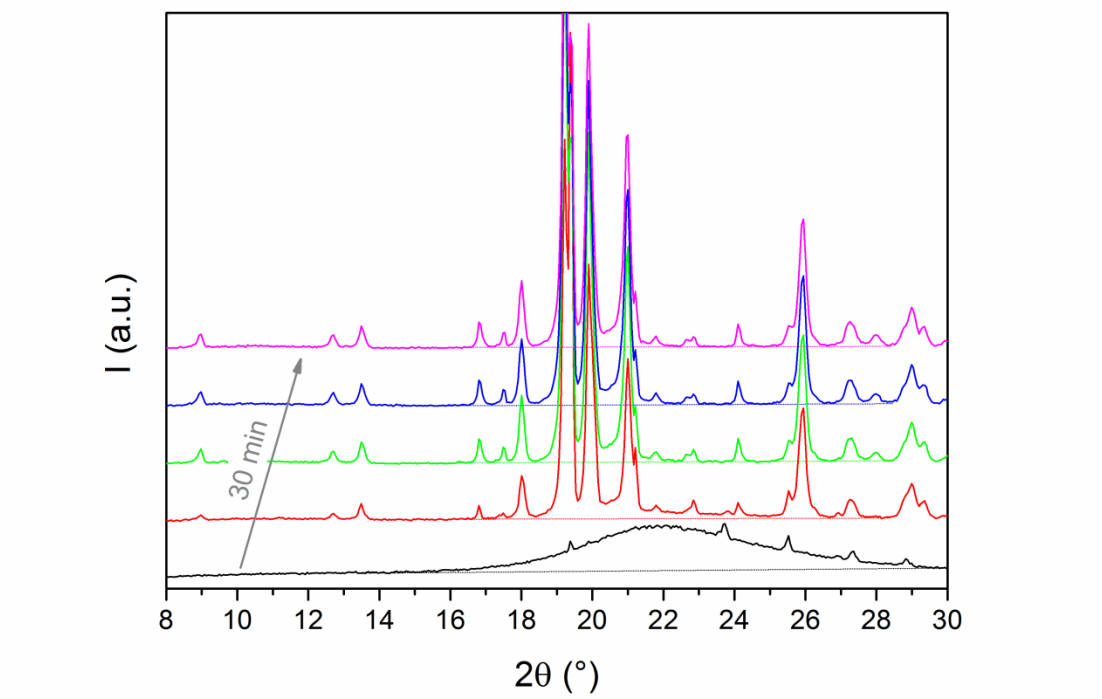

Figure S1 Evolution of the WAXS diffractogram of TR at T = – 40 °C, observing complete crystallization of the sample after 30 min. The baselines should guide the eye.

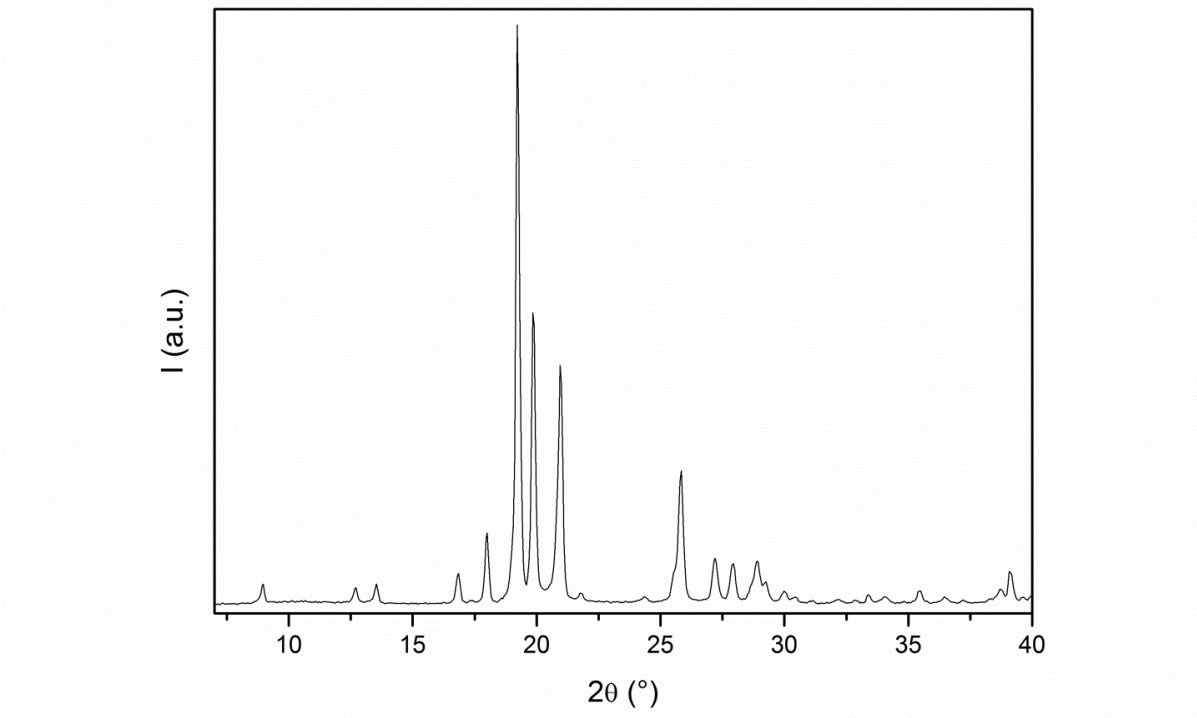

Figure S2 WAXS diffractogram of 1,2,3-triazole at T = – 15 °C in the range of 7° < 2θ < 40°.

Table S1 Evaluation of the WAXS diffractogram and assignment of the reflexes of 1,2,3-triazole at T = – 15 °C.

2θ (°)	I (counts)	I_{rel} (%)	d (Å)	d^{-2} (Å^{-2})	*Index* h	k	l	d_{cal} (Å)	d_{cal}^{-2} (Å^{-2})	d-d_{cal} (Å)	d^{-2} - d_{cal}^{-2} (Å^{-2})
8.95	1664	3.4	9.883	0.010	2	0	0	9.843	0.010	0.040	0.000
12.69	1289	2.6	6.976	0.021	$\bar{2}$	0	1	6.973	0.021	0.003	0.000
13.53	1595	3.2	6.544	0.023	2	0	1	6.541	0.023	0.003	0.000
16.83	2679	5.4	5.267	0.036	1	1	0	5.257	0.036	0.010	0.000
17.99	6249	12.7	4.930	0.041	4	0	0	4.921	0.041	0.009	0.000
19.24	49249	100.0	4.614	0.047	$\bar{1}$	1	1	4.634	0.047	-0.020	0.000
19.87	26177	53.2	4.467	0.050	$\bar{4}$	0	1	4.467	0.050	0.000	0.000
20.95	20036	40.7	4.240	0.056	4	0	1	4.237	0.056	0.003	0.000
21.78	643	1.3	4.080	0.060	2	0	2	4.189	0.057	-0.109	0.003
24.35	407	0.8	3.655	0.075	4	1	0	3.654	0.075	0.001	0.000
25.55	2397	4.9	3.486	0.082	$\bar{4}$	0	2	3.506	0.081	-0.020	0.001
25.82	11570	23.5	3.450	0.084	1	1	2	3.456	0.084	-0.006	0.000
27.20	3706	7.5	3.279	0.093	2	1	2	3.273	0.093	0.006	0.000
27.92	3299	6.7	3.196	0.098	5	1	0	3.175	0.099	0.021	-0.001
28.89	3202	6.5	3.091	0.105	$\bar{5}$	0	2	3.068	0.106	0.023	-0.002
29.26	1352	2.7	3.052	0.107	3	1	2	3.048	0.108	0.004	0.000
29.99	975	2.0	2.980	0.113	5	1	1	2.971	0.113	0.009	-0.001
32.87	226	0.5	2.725	0.135	3	0	3	2.727	0.134	-0.002	0.000
33.40	713	1.4	2.683	0.139	$\bar{1}$	1	3	2.688	0.138	-0.005	0.001
35.46	1046	2.1	2.532	0.156	$\bar{3}$	1	3	2.537	0.155	-0.005	0.001

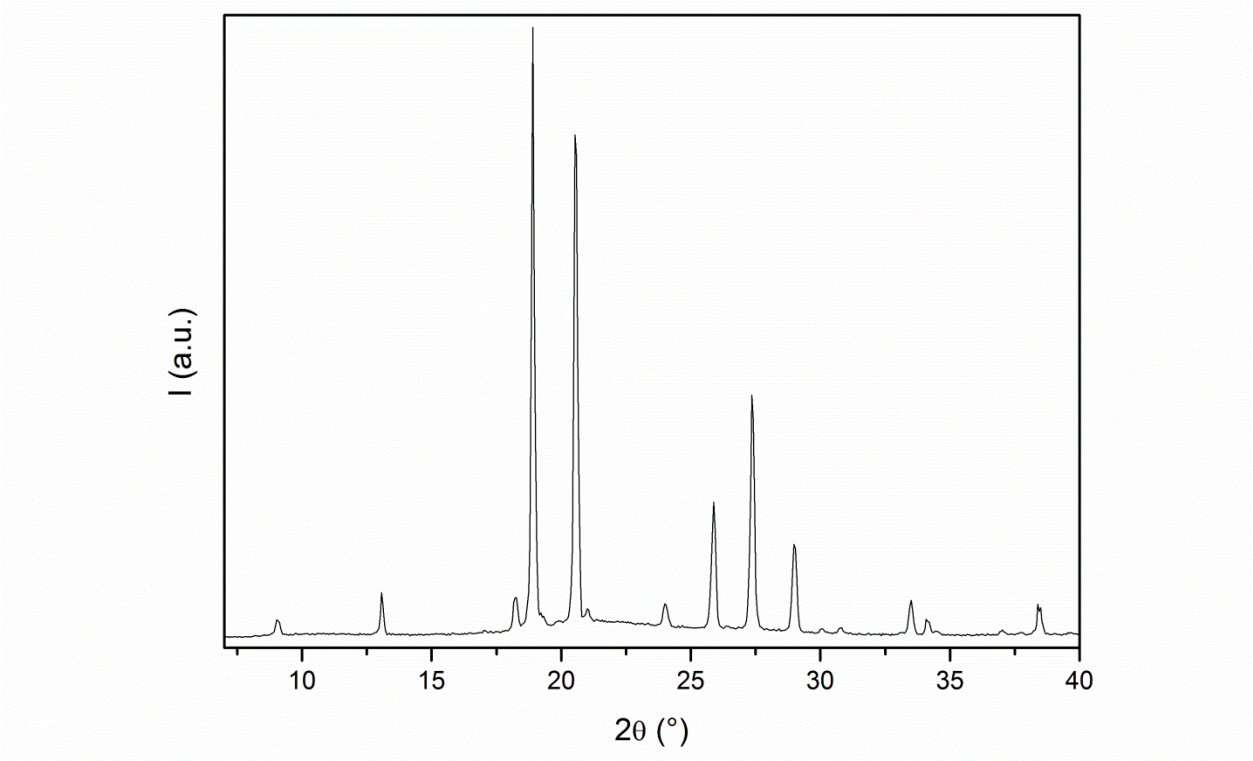

Figure S3 WAXS diffractogram of 1,2,3-triazole at T = 10 °C in the range of 7° < 2θ < 40°.

Table S2 Evaluation of the WAXS diffractogram and assignment of the reflexes of 1,2,3-triazole at T = 10 °C.

2θ (°)	I (counts)	I_{rel} (%)	d (Å)	d^{-2} (Å^{-2})	Index h	k	l	d_{cal} (Å)	d_{cal}^{-2} (Å^{-2})	d-d_{cal} (Å)	d^{-2} - d_{cal}^{-2} (Å^{-2})
9.07	1287	2.8	9.755	0.011	0	2	0	9.686	0.011	0.069	0.000
13.08	3306	7.2	6.767	0.022	1	2	0	6.720	0.022	0.047	0.000
18.24	1967	4.3	4.864	0.042	0	4	0	4.843	0.043	0.021	0.000
18.91	45813	100.0	4.693	0.045	2	0	0	4.665	0.046	0.027	-0.001
20.56	40955	89.4	4.320	0.054	1	4	0	4.298	0.054	0.021	-0.001
21.02	761	1.7	4.226	0.056	2	2	0	4.203	0.057	0.023	-0.001
24.02	1879	4.1	3.705	0.073	0	1	1	3.633	0.076	0.072	-0.003
25.88	10083	22.0	3.443	0.084	1	1	1	3.385	0.087	0.057	-0.003
27.38	19012	41.5	3.258	0.094	0	3	1	3.209	0.097	0.049	-0.003
29.00	7354	16.1	3.079	0.105	1	3	1	3.035	0.109	0.044	-0.003
30.06	350	0.8	2.972	0.113	3	2	0	2.961	0.114	0.011	-0.001
30.78	474	1.0	2.905	0.118	2	1	1	2.866	0.122	0.039	-0.003
33.49	2651	5.8	2.675	0.140	2	3	1	2.644	0.143	0.031	-0.003
34.13	1263	2.8	2.627	0.145	3	4	0	2.617	0.146	0.010	-0.001

34.47	291	0.6	2.602	0.148	1	5	1	2.572	0.151	0.030	-0.003
37.02	344	0.8	2.428	0.170	0	8	0	2.422	0.171	0.007	-0.001
37.73	163	0.4	2.384	0.176	3	1	1	2.363	0.179	0.021	-0.003
38.37	4314	9.4	2.346	0.182	1	8	0	2.344	0.182	0.002	-0.000
38.46	2020	4.4	2.340	0.183	4	0	0	2.333	0.184	0.008	-0.001
39.63	144	0.3	2.274	0.193	4	2	0	2.268	0.194	0.006	-0.001

Table S3 Refined atom positions and bond lengths of the low temperature modification of TR at $T = -15$ °C. For assignment of the atoms see the molecular complex in Figure S4 (c).

Atom	***Position***		
	x	***y***	***z***
N1	0.4054	0.0075	0.9324
C2	0.4431	0.2042	0.9060
N3	0.4038	0.0435	0.7050
C4	0.4421	0.2273	0.7601
N5	0.2230	0.8419	1.0919
C6	0.2611	0.6606	1.1494
N7	0.2276	0.8766	1.3329
C8	0.2639	0.6819	1.2977
N9	0.3810	– 0.0914	0.8098
N10	0.2043	0.9627	1.2063
N11	0.5707	1.1006	– 0.2161
C12	0.6064	0.9202	– 0.2728
N13	0.5616	1.1498	– 0.4428
C14	0.6006	0.9518	– 0.4182
N15	0.5430	1.2415	– 0.3196
H16	0.1709	3.1227	1.1923
H17	0.4682	0.3133	0.9995
H18	0.3902	– 0.0042	0.5906
H19	0.4661	0.3631	0.6851
H20	0.2848	0.5212	1.0763
H21	0.2908	0.5657	1.3860
H22	0.5623	1.1416	– 0.1014
H23	0.6339	0.7802	– 0.1991
H24	0.6213	0.8482	– 0.5126

Bond	***Lengths* (Å)**
N1 - N9	1.32
N1 - C2	1.34
C2 - C4	1.36
C2 - H17	1.14
N3 - N9	1.32
N3 - C4	1.34
N3 - H18	1.11
C4 - H19	1.14
N5 - N10	1.32
N5 - C6	1.33
C6 - C8	1.38
C6 - H20	1.14
N7 - N10	1.32
N7 - C8	1.33
C8 - H21	1.14
N10 - H16	1.10
N11 - N15	1.32
N11 - C12	1.34
N11 - H22	1.11
C12 - C14	1.36
C12 - H23	1.14
N13 - N15	1.32
N13 - C14	1.34
C14 - H24	1.14
H16 - N10	1.10

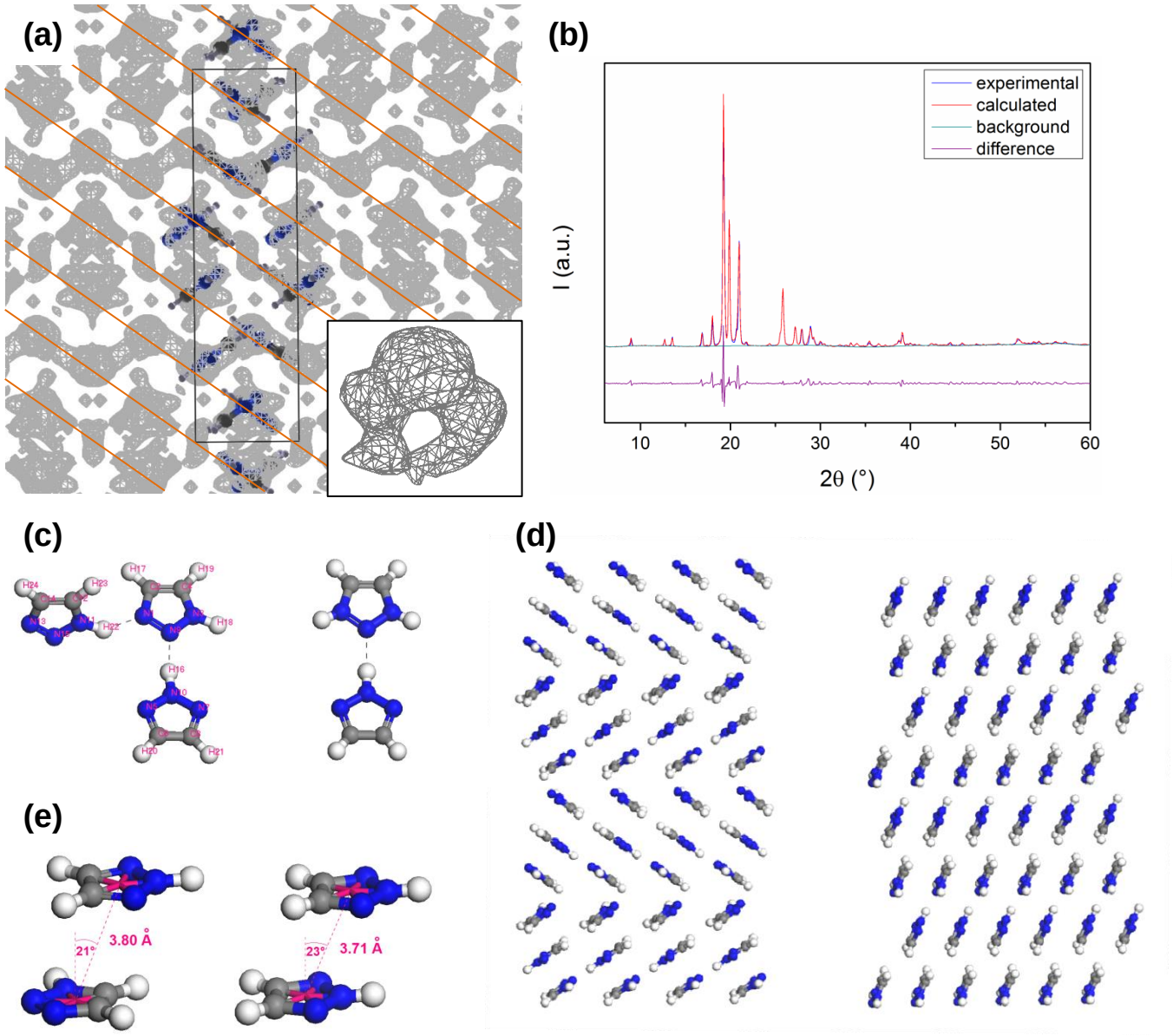

Figure S4 (a) Unrefined Fourier map of the electron density in the monoclinic unit cell of TR at $T = -15$ °C, the positions of the TR molecules as used for the refinement of the data is deposited. The orange lines are the (510) planes and the inset shows the electron density conture of a pentagon. (b) Experimental WAXS trace of the low temperature modification of TR at $T = -15$ °C and the simulated trace after Rietvelt refinement (R_p = 9.39 %, R_{wp} = 14.28 %) using BIOVIA Materials Studio Reflex software. The difference of the experimental and simulated diffractograms is additionally shown. (c) Comparison of the 2:1 molecular complex (1*H*:2*H*) of the monoclinic (left) and 1:1 molecular complex of the orthorhombic modification. The atoms are labeled for the assignment of the positions and bond lengths in Table S3. (d) Comparison of the π-π stacks of the low temperature modification (left) and the high temperature modification (right). (e) Centroid-centroid distance between two TR molecules in the monoclinic (left) and orthorhombic modification (right).

Determination of Conductivity and Relaxation Time from Impedance Data

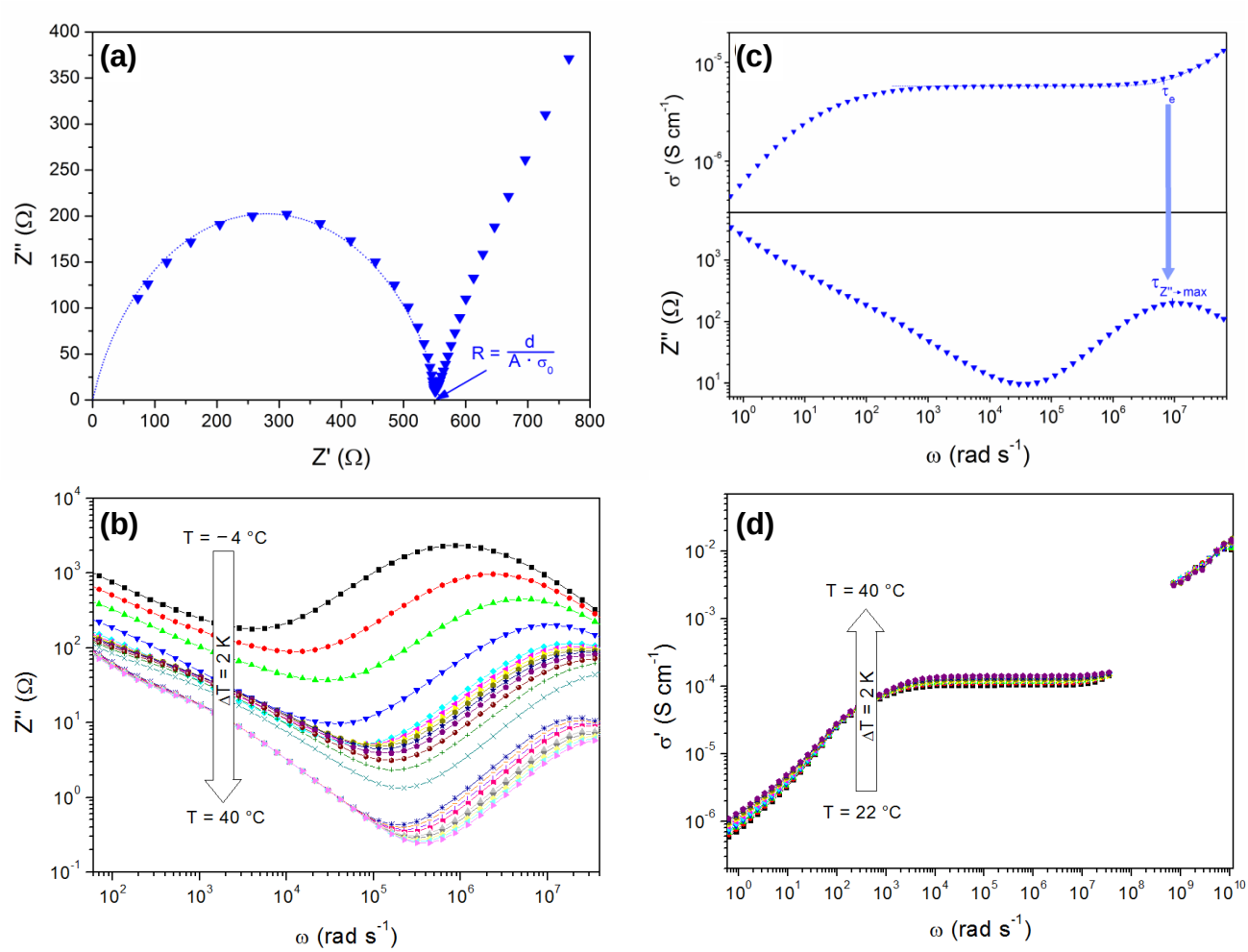

Figure S5 (a) Nyquist plot of 1,2,3-triazole at T = 2 °C (blue curve of Fig. 4 (a)). The arrow shows the bulk resistance R which can be used for the calculation of the dc conductivity. (b) Imaginary part of the complex impedance as function of the angular frequency between T = – 4 °C and T = 40 °C in steps of ΔT = 2 K. (c) Agreement of the characteristic relaxation time (τ_e), obtained by fitting the conductivity data with the Dyre function (eq. 2) with the relaxation time of the maximum in the imaginary part of the complex impedance as function of the angular frequency ($\tau_{Z''\rightarrow max}$)at T = 2 °C. (d) Same as Fig. 4 (a) for temperatures between T = 22 °C and T = 40 °C in steps of ΔT = 2 K. The high frequency data ($5 \cdot 10^7$ Hz ≤ $\nu \leq 1.8 \cdot 10^9$ Hz) measured with the HP impedance analyzer in a Novocontrol RF sample cell (diameter: 3 mm; sample thickness: 1 mm) are added. Due to inductive effects, it is not possible to obtain correct data below $\nu \geq 5 \cdot 10^7$ Hz with this sample cell ('frequency gap'). Small deviations of σ' are possible due to the different sample cell geometries. The high frequency region shows a steady increase and no further relaxation above $\omega > \omega_e$.

Pulsed field gradient nuclear magnetic resonance (PFG NMR)

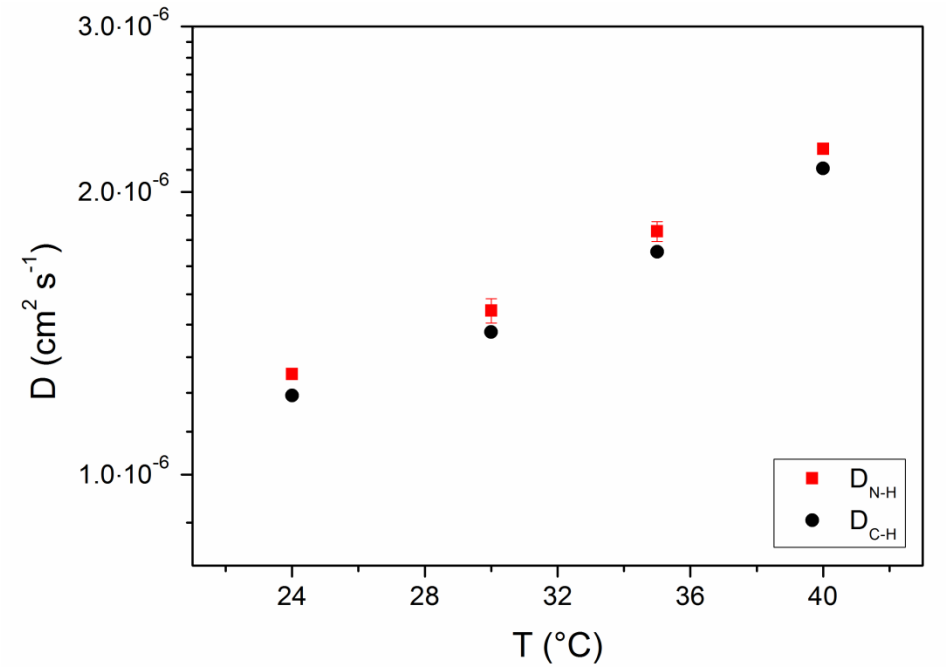

Figure S6 Diffusion coefficients, measured with PFG NMR spectroscopy. The diffusion coefficients of the acidic N-H and aromatic C-H proton are received by separate integration of the corresponding signals.

Barton–Nakajima–Namikawa relation and relaxation time

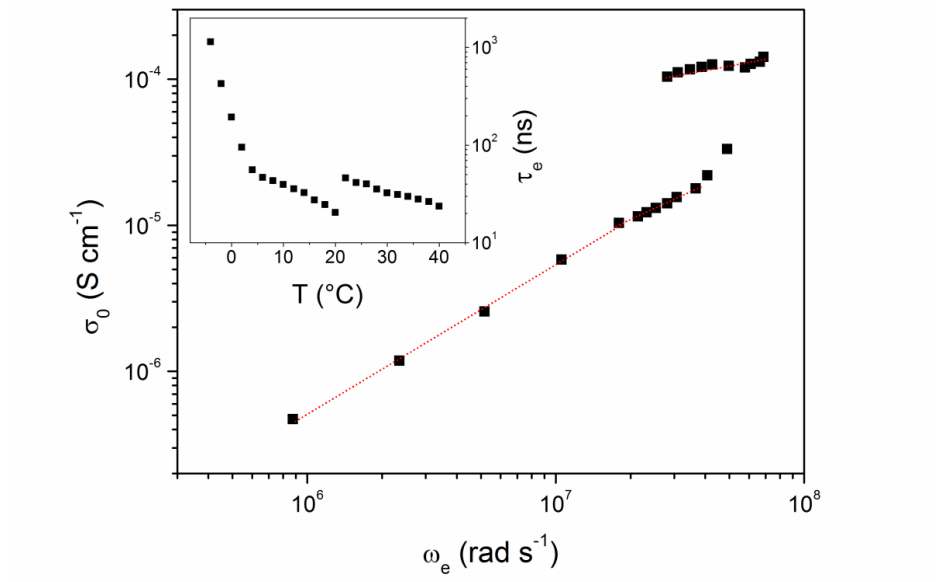

Figure S7 Proton conductivity of 1,2,3-triazole as function of the characteristic angular frequency of the Dyre formula. The inset shows the temperature dependence of the relaxation time ($\tau_e = 1 / \omega_e$).

Explanation of the separation of the proton conductivity (Figure 7)

The proton conductivity is given by eq. 10:

$$\sigma_0 = \frac{F^2 \cdot c_0}{R \cdot T}\left(D_{hopp} \cdot H_R^{-1} + 2 \cdot D_{vehicle} \cdot \alpha_{vehicle}\right) \tag{10}$$

Proton hopping is known as random process but only the transport of charges can contribute to the proton conductivity. The physical quantity which describes the proportion of actively contribution hopping charge carriers is the inverse Haven ratio H_R^{-1}. However, the number of charges for proton hopping is also limited to a degree of dissociation α_{hopp}. Replacing H_R^{-1} by α_{hopp} yields

$$\frac{R \cdot T \cdot \sigma_0}{F^2 \cdot c_0} = D_{hopp} \cdot \alpha_{hopp} + 2 \cdot D_{vehicle} \cdot \alpha_{vehicle} \tag{S1}$$

In the limit of $T \rightarrow 30°C$, $D_{vehicle}$ can be approximated by

$$D_{vehicle} = D_{vehicle}\big|_{T=30°C} + \left.\frac{\partial D_{vehicle}}{\partial D_{hopp}}\right|_{T=30°C} \cdot \left(D_{hopp} - D_{hopp}\big|_{T=30°C}\right) \tag{S2}$$

And then eq. S1 turns into

$$\frac{R \cdot T \cdot \sigma_0}{F^2 \cdot c_0} = \left(\alpha_{hopp} + \left.\frac{\partial\left(2\,\alpha_{vehicle}\, D_{vehicle}\right)}{\partial D_{hopp}}\right|_{\substack{T= \\ 30°C}}\right) \cdot D_{hopp} + 2\left(\alpha_{vehicle}\, D_{vehicle} - \frac{\partial\left(\alpha_{vehicle} D_{vehicle}\right)}{\partial D_{hopp}}\, D_{hopp}\right)\Bigg|_{\substack{T= \\ 30°C}} \tag{S3}$$

Since the temperature dependence of $D_{vehicle}$ is much smaller compared to D_{hopp} (see discussion around eq. 5 and eq. 11), the partial derivative is negligible small and eq. S3 simplifies to

$$\frac{R \cdot T \cdot \sigma_0}{F^2 \cdot c_0} = \alpha_{hopp} \cdot D_{hopp} + 2 \cdot \left(\alpha_{vehicle}\, D_{vehicle}\right)\big|_{T=30°C} \tag{S4}$$

Using again inverse Haven ratio H_R^{-1} then eq. S4 turns into eq. 12

$$\frac{R \cdot T \cdot \sigma_0}{F^2 \cdot c_0} = D_{hopp} \cdot H_R^{-1} + 2 \cdot \left(\alpha_{vehicle}\, D_{vehicle}\right)\big|_{T=30°C} \tag{12}$$

This mathematical derivation can also be confirmed by experimental values which are shown in Fig. S8. The intrinsic conductivity and its contributions to the two mechanisms are plotted considering the temperature dependence of D_{hopp} and $D_{vehicle}$ (assuming Arrhenius behavior, Fig. 6 and Fig. S6). The calculated error for the inverse Haven ratio from the consideration of the temperature dependence of $D_{vehicle}$ is in the same range as the error of the linearization ($H_R^{-1} = (1.1 \pm 0.1) \cdot 10^{-2}$). Thus, the averaged degree of dissociation at $T = 30$ °C is $\alpha_{vehicle} = (3.5 \pm 0.4) \cdot 10^{-4}$.

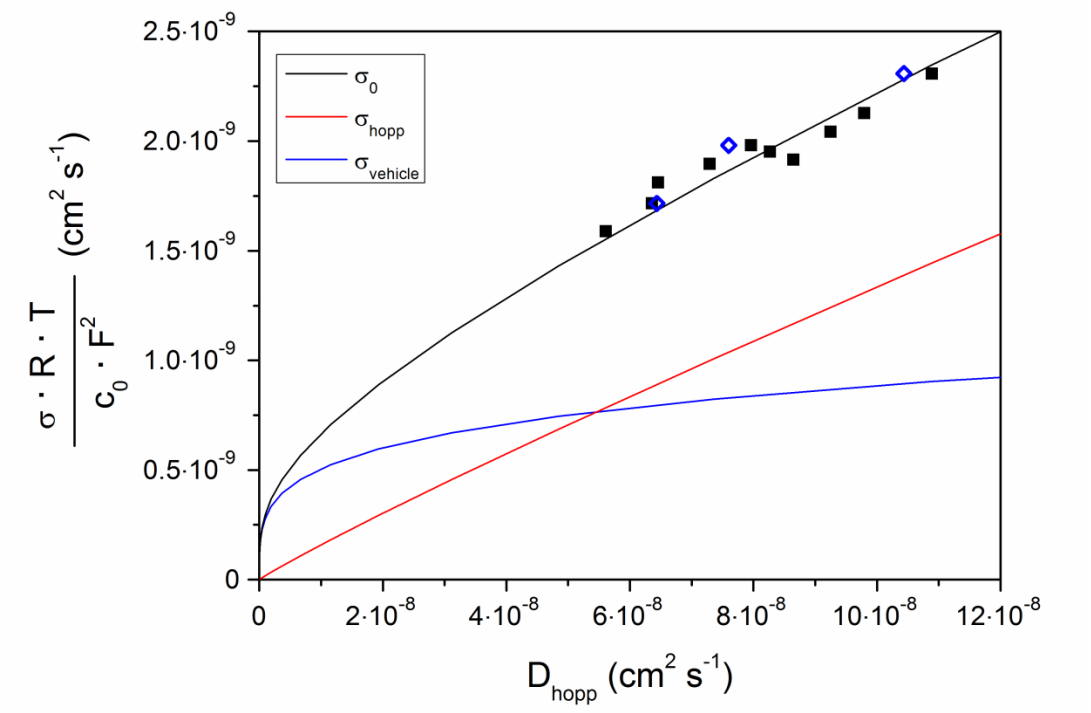

Figure S8 Intrinsic conductivity and the contributions to the two mechanisms as function of the hopping diffusion coefficient.

Dielectric constant

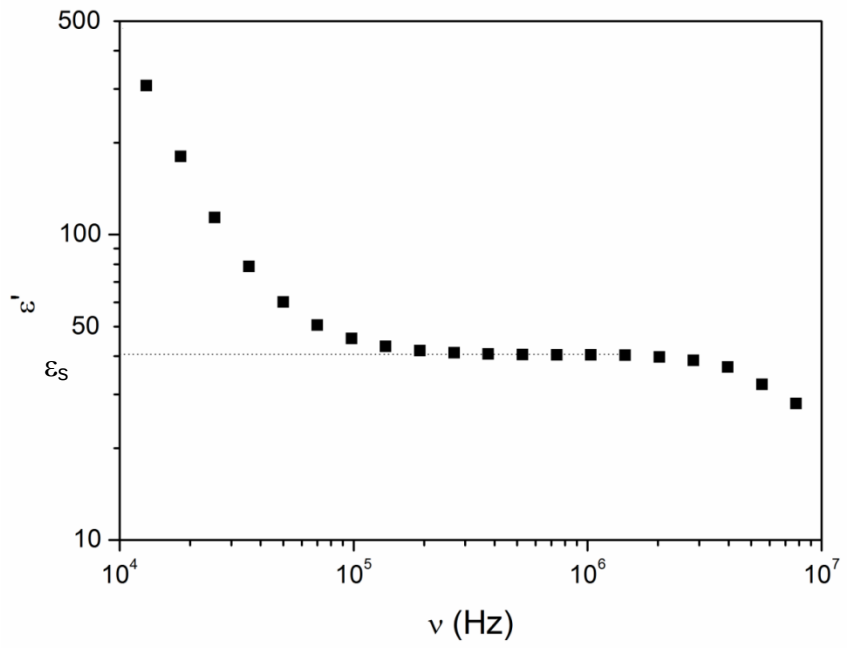

Figure S9 Real part of the complex dielectric function as function of the frequency at T = 24 °C for determination of the dielectric constant ε_s.